

Post-Insemination Selection Dominates Pre-Insemination Selection in Driving Rapid Evolution of Male Competitive Ability --Manuscript Draft--

Manuscript Number:	PGENETICS-D-21-00891
Full Title:	Post-Insemination Selection Dominates Pre-Insemination Selection in Driving Rapid Evolution of Male Competitive Ability
Short Title:	Post-Insemination Selection Drives Male Evolution
Article Type:	Research Article
Section/Category:	Evolution
Keywords:	experimental evolution, sexual selection, reproductive success, genomics, <i>Caenorhabditis elegans</i>
Abstract:	Sexual reproduction is a complex process that contributes to differences between the sexes and divergence between species. From a male's perspective, sexual selection can optimize reproductive success by acting on the variance in mating success (pre-insemination selection) as well as the variance in fertilization success (post-insemination selection). The balance between pre- and post-insemination selection has not yet been investigated using a strong hypothesis-testing framework that directly quantifies the effects of post-insemination selection on the evolution of reproductive success. Here we use experimental evolution of a uniquely engineered genetic system that allows sperm production to be turned off and on in obligate male-female populations of <i>Caenorhabditis elegans</i> . We show that enhanced post-insemination competition increases the efficacy of selection and surpasses pre-insemination sexual selection in driving a polygenic response in male reproductive success. We find that after 30 generations post-insemination selection increased male reproductive success by an average of 5- to 7-fold. Contrary to expectation, enhanced pre-insemination competition hindered selection and slowed the rate of evolution. Furthermore, we found that post-insemination selection resulted in a strong polygenic response at the whole-genome level. Our results demonstrate that post-insemination sexual selection plays a critical role in the rapid optimization of male reproductive fitness. Therefore, explicit consideration should be given to post-insemination dynamics when considering the population effects of sexual selection.
Additional Information:	
Question	Response
<p>Financial Disclosure</p> <p>Enter a financial disclosure statement that describes the sources of funding for the work included in this submission. Review the submission guidelines for detailed requirements. View published research articles from PLOS Genetics for specific examples.</p> <p>This statement is required for submission and will appear in the published article if the submission is accepted. Please make sure it is accurate.</p>	<p>This work was funded by National Institutes of Health grant R35GM131838 to PCP (https://grants.nih.gov/grants/guide/pa-files/PAR-17-094.html). KRK is supported by a Natural Sciences and Engineering Research Council of Canada Banting Postdoctoral Fellowship (https://banting.fellowships-bourses.gc.ca/en/2019-2020-eng.html). The funders had no role in study design, data collection and analysis, decision to publish, or preparation of the manuscript.</p>

Unfunded studies

Enter: *The author(s) received no specific funding for this work.*

Funded studies

Enter a statement with the following details:

- Initials of the authors who received each award
- Grant numbers awarded to each author
- The full name of each funder
- URL of each funder website
- Did the sponsors or funders play any role in the study design, data collection and analysis, decision to publish, or preparation of the manuscript?
- **NO** - Include this sentence at the end of your statement: *The funders had no role in study design, data collection and analysis, decision to publish, or preparation of the manuscript.*
- **YES** - Specify the role(s) played.

* typeset

Competing Interests

Use the instructions below to enter a competing interest statement for this submission. On behalf of all authors, disclose any [competing interests](#) that could be perceived to bias this work—acknowledging all financial support and any other relevant financial or non-financial competing interests.

This statement **will appear in the published article** if the submission is accepted. Please make sure it is accurate. View published research articles from [PLOS Genetics](#) for specific examples.

The authors have declared that no competing interests exist.

NO authors have competing interests

Enter: *The authors have declared that no competing interests exist.*

Authors with competing interests

Enter competing interest details beginning with this statement:

I have read the journal's policy and the authors of this manuscript have the following competing interests: [insert competing interests here]

* typeset

This statement is **required** for submission and **will appear in the published article** if the submission is accepted. Please make sure it is accurate and that any funding sources listed in your Funding Information later in the submission form are also declared in your Financial Disclosure statement.

Data Availability

Authors are required to make all data underlying the findings described fully available, without restriction, and from the time of publication. PLOS allows rare exceptions to address legal and ethical concerns. See the [PLOS Data Policy](#) and [FAQ](#) for detailed information.

A Data Availability Statement describing where the data can be found is required at submission. Your answers to this question constitute the Data Availability Statement and will be published in the article, if accepted.

Yes - all data are fully available without restriction

Important: Stating 'data available on request from the author' is not sufficient. If your data are only available upon request, select 'No' for the first question and explain your exceptional situation in the text box.

Do the authors confirm that all data underlying the findings described in their manuscript are fully available without restriction?

Describe where the data may be found in full sentences. If you are copying our sample text, replace any instances of XXX with the appropriate details.

- If the data are **held or will be held in a public repository**, include URLs, accession numbers or DOIs. If this information will only be available after acceptance, indicate this by ticking the box below. For example: *All XXX files are available from the XXX database (accession number(s) XXX, XXX).*
- If the data are all contained **within the manuscript and/or Supporting Information files**, enter the following: *All relevant data are within the manuscript and its Supporting Information files.*
- If neither of these applies but you are able to provide **details of access elsewhere**, with or without limitations, please do so. For example:

Data cannot be shared publicly because of [XXX]. Data are available from the XXX Institutional Data Access / Ethics Committee (contact via XXX) for researchers who meet the criteria for access to confidential data.

The data underlying the results presented in the study are available from (include the name of the third party and contact information or URL).

- This text is appropriate if the data are owned by a third party and authors do not have permission to share the data.

The oligonucleotides and synthetic constructs used in this study are available as Supplemental Tables S1-S3. The sequence data will be made publicly available on NCBI prior to publication. Model summary statistics for the genomic analyses (Files S1-S6) and the fertility data (File S7) are available in the Figshare repository <https://figshare.com/s/735e8011f9a1239a5c85>, which will be made public upon acceptance. All R scripts are available via the GitHub repository https://github.com/katjakasimatis/postinsemination_expevol. Worm strains PX624, PX631, and PX658 will be made available from the Caenorhabditis Genetics Center. All other strains are available from the Phillips Lab upon request.

* typeset	
Additional data availability information:	Tick here if the URLs/accession numbers/DOIs will be available only after acceptance of the manuscript for publication so that we can ensure their inclusion before publication.



1 Post-Insemination Selection Dominates Pre-Insemination Selection in Driving Rapid Evolution
2 of Male Competitive Ability

3

4

5

Short Title: Post-Insemination Selection Drives Male Evolution

6

7

8 Katja R. Kasimatis^{1,#a*}, Megan J. Moerdyk-Schauwecker¹, Ruben Lancaster¹, Alexander Smith¹,
9 John H. Willis¹, and Patrick C. Phillips^{1*}

10

11 ¹Institute of Ecology and Evolution, University of Oregon, Eugene, Oregon, United States of
12 American

13

14 ^{#a}Current address: Department of Ecology and Evolutionary Biology, University of Toronto,
15 Toronto, Ontario, Canada

16

17 *Corresponding authors:

18 Email: k.kasimatis@utoronto.ca (KRK)

19 Email: pphil@uoregon.edu (PCP)

20

21 **Abstract**

22 Sexual reproduction is a complex process that contributes to differences between the sexes and
23 divergence between species. From a male’s perspective, sexual selection can optimize
24 reproductive success by acting on the variance in mating success (pre-insemination selection) as
25 well as the variance in fertilization success (post-insemination selection). The balance between
26 pre- and post-insemination selection has not yet been investigated using a strong hypothesis-
27 testing framework that directly quantifies the effects of post-insemination selection on the
28 evolution of reproductive success. Here we use experimental evolution of a uniquely engineered
29 genetic system that allows sperm production to be turned off and on in obligate male-female
30 populations of *Caenorhabditis elegans*. We show that enhanced post-insemination competition
31 increases the efficacy of selection and surpasses pre-insemination sexual selection in driving a
32 polygenic response in male reproductive success. We find that after 30 generations post-
33 insemination selection increased male reproductive success by an average of 5- to 7-fold.
34 Contrary to expectation, enhanced pre-insemination competition hindered selection and slowed
35 the rate of evolution. Furthermore, we found that post-insemination selection resulted in a strong
36 polygenic response at the whole-genome level. Our results demonstrate that post-insemination
37 sexual selection plays a critical role in the rapid optimization of male reproductive fitness.
38 Therefore, explicit consideration should be given to post-insemination dynamics when
39 considering the population effects of sexual selection.

40

41 **Author Summary**

42 Some of the most dramatic and diverse phenotypes observed in nature—such as head-butting in
43 wild sheep and the elaborate tails of peacocks—are between the sexes. These remarkable
44 phenotypes are a result of sexual selection optimizing reproductive success in females and males
45 independently. For males, total reproductive success is comprised of winning a mating event and
46 then translating that mating event into a fertilization event. Therefore, to understand not only
47 how male reproductive success is comprised, but also how it evolves, we must examine the
48 interaction between pre- and post-insemination sexual selection. We combine environmentally-
49 inducible control of sperm production within a highly reproducible factorial experimental
50 evolution design to directly quantify the contribution of post-insemination selection to male

51 reproductive evolution. We demonstrate that enhanced sperm competition increases the efficacy
52 of selection and enhances the rate of male evolution. Alternatively, we show that enhanced pre-
53 insemination competition slows the evolutionary rate. Using whole-genome approaches, we
54 identify over 60 genes that contribute to male fertilization success. Brought together, our new
55 approaches and results demonstrate that the unseen world of molecular interactions occurring
56 during post-insemination are as fundamentally important as the pre-mating factors that lead to
57 some of the most fascinating traits.

58

59 **Introduction**

60 Sexual selection drives the evolution of some of the most remarkable phenotypes observed in
61 nature. Interest in these flashy phenotypes has led to a focus on studying pre-insemination
62 reproductive dynamics, such as male-male competition and female choice [1]. However, in
63 animals with internal fertilization, reproduction is more complex and requires a series of
64 interactions within and between the sexes to produce a viable offspring. From a male's
65 perspective, total reproductive success can be partitioned into successfully winning a mating
66 event and then successfully winning a fertilization event. Therefore, sexual selection has the
67 potential to act on both the variance in mating success and the variance in fertilization success
68 (also referred to as gametic selection [2,3]). We do not know how selection during these
69 reproductive phases interacts in an additive, antagonistic, or synergistic manner to optimize total
70 male reproductive success. Understanding this balance is critical not only for quantifying male
71 reproductive fitness within a generation, but also for understanding how sexual selection shapes
72 the evolution of reproductive success over time. Such processes are critical for relating the role
73 of sexual selection to population adaptation [4,5] and divergence [6].

74 Experimental separation of sexual selection before and after mating within an adaptive
75 framework has proved extremely challenging. Previous studies have taken the approach of
76 Arnold and Wade [7] to partition the variance in total reproductive success into the variance in
77 mating success and the variance in fertilization success [reviewed in 8]. These studies have
78 inferred mixed results as to opportunity for sexual selection. Several studies suggest that the
79 variance in mating success comprises greater than 95% of the total variance in reproductive
80 success [9,10], while others indicate a greater contribution of the post-insemination phase [11-
81 15]. Additionally, evolutionary analyses of seminal fluid proteins show a high opportunity for

82 post-insemination selection [16,17]. While informative, the opportunity for sexual selection does
83 not necessarily translate into realized selection, which contributes to the lack of consistent
84 patterns between studies. Moreover, this framework is an indirect approach for partitioning
85 reproductive success and thus lacks the ability to connect the action of selection to the
86 underlying genomic response to understand how reproductive success is evolving.

87 *Caenorhabditis elegans* is an ideal system for disentangling mating interactions. First, the
88 mating system in *C. elegans* can be manipulated to prevent hermaphrodite self-sperm production
89 and create functional females that rely on male-female mating. Males in these populations have
90 low reproductive success relative to males from obligate outcrossing *Caenorhabditis* species
91 [18], which creates a high opportunity for the evolution of reproductive success. Second, we
92 have developed an external, non-toxic sterility system for *C. elegans* [19] that capitalizes on the
93 auxin-inducible degron system to degrade the critical spermatogenesis gene *spe-44* and
94 effectively turn off sperm production. The induction of sterility allows for sperm competitive
95 dynamics to be isolated from male-male competitive dynamics for thousands of worms at a time.
96 Finally, *C. elegans* is amenable to the evolve and re-sequence experimental approach [20,21],
97 which allows us to not only quantify the impact of sexual selection on reproductive success, but
98 also identify the underlying genetic structure of the traits involved.

99 Here we capitalize on transgenics to isolate the contributions of pre-insemination mating
100 competition versus post-insemination sperm competition to the evolution of reproductive fitness
101 of a newly derived *C. elegans* male population. We first create an obligate outcrossing *C.*
102 *elegans* population composed of functional females and males with inducible sterility. We then
103 performed 30 generations of replicated experimental evolution using a factorial design that
104 partitions sexual selection due to within-strain and between-strain competitive dynamics
105 occurring during pre-insemination and post-insemination. This experiment explicitly tests if pre-
106 insemination sexual selection and post-insemination sexual selection contribute to reproductive
107 success in an additive, synergistic, or antagonistic manner. If pre- and post-insemination
108 selection are additive or synergistic, then we expect to see the greatest increase in total
109 reproductive success when competition is enhanced through the addition of external male
110 competitors during both reproductive stages. Alternatively, if these phases are antagonistic such
111 that competition is beneficial during one stage but detrimental during the other, then we expect to
112 see a reduction in total reproductive success when competition is enhanced during both

113 reproductive stages. We can infer the source of antagonistic competition by comparing-and-
114 contrasting the effects of enhanced and reduced post-insemination competition.

115

116 **Results**

117 **Factorial framework to isolate selection on mating and fertilization** 118 **success**

119 We designed an experimental evolution framework that controls pre- and post-insemination
120 competitive interactions using three distinct and powerful genetic manipulations: a mutation in
121 the sex determination pathway (*fog-2*) to disrupt self-sperm production in hermaphrodites and
122 maintain obligate male-female mating [18], targeted degradation of a key spermatogenesis
123 protein (*spe-44*) to control male mating duration [19], and an inducible lethal marker (*peel-1*) to
124 eliminate offspring from competitor males [22]. To generate a selective event, male sterility was
125 induced after an initial mating period (Fig 1). Increased sperm competition was then generated
126 by adding competitor males from a different strain. After a 24 hour competitive phase, progeny
127 were collected, hatched, and then heat-shocked to induce lethality of the competitor male cross-
128 progeny, leaving only those progeny from the evolving males to start the next generation. This
129 design isolates sperm competitive success from male mating success and selects for sperm
130 defensive capability and longevity.

131 The induction of sterility and addition of competitor males generated a factorial
132 experimental design resulting in four experimental evolution regimes (Fig 2A). When both
133 sterility was introduced and competitors subsequently added (between-strain post-insemination
134 only competition, BS-PO), there was increased sexual selection on post-insemination fertilization
135 dynamics. Alternatively, when only sterility was induced, and competitor males not added
136 (within-strain post-insemination only competition, WS-PO), evolving males experienced reduced
137 sperm competition and potentially decreased post-insemination sexual selection. To represent the
138 full degree of sexual selection acting on pre- and post-insemination competition (between-strain
139 pre- and post-insemination competition, BS-P&P), sterility was not induced, but competitor
140 males were added. Finally, no direct sexual selection was applied when neither sterility was
141 induced nor competitors added (within-strain pre- and post-insemination competition, WS-P&P).

142 The WS-P&P regime represents the base level of sexual selection experienced by recently
143 derived *C. elegans* males.

144 **Opportunity for selection is high in the ancestral population**

145 We used multiple rounds of low-dose EMS mutagenesis to generate genetic variation in the
146 ancestral population (Fig S1). Based on the mutation rate of EMS per generation [23], at least
147 937,500 non-exclusive mutations were expected to be segregating in the post-mutagenesis
148 population prior to lab adaptation. We observed 321,929 SNPs segregating in the ancestral
149 population, suggesting strong purifying selection during the pre-experimental evolution lab
150 adaptation period (Fig S1). The ancestral population had a genome-wide mean nucleotide
151 diversity of $\pi = 0.06$ and the minor allele frequency ranged from 0.004 to 0.5 (Fig S2A-D; File
152 S1). These diversity estimates are higher than those commonly observed in *C. elegans* and are
153 more comparable to the obligate outcrossing species *C. remanei* [24]. The distribution of variants
154 was relatively even across chromosome domains, unlike the characteristic pattern of higher
155 diversity on the chromosome arms when compared to the chromosome center [25-27] (Fig S2C-
156 D; File S2). SNP density, however, reflected this chromosome arm-center pattern: the mean SNP
157 density on chromosome arms was $\theta_w = 0.004$ and in chromosome centers was $\theta_w = 0.002$ (Fig
158 S2E-F). Despite the X chromosome having a slightly higher recombination rate in the small
159 chromosome center domain [25] coupled with a greater opportunity for purifying selection in
160 males, the X did not have the lowest SNP density (mean $\theta_w = 0.0027$) as expected. Instead,
161 chromosome I had a significantly lower mean SNP density (mean $\theta_w = 0.0012$; $t = -67$, $p <$
162 0.001) than the other chromosomes. Together these summary statistics indicate that the ancestral
163 population had more segregating genetic variants than is commonly observed in *C. elegans*,
164 though much of this diversity is not in the gene dense chromosome centers.

165 We quantified ancestral reproductive success under highly competitive conditions
166 occurring during both pre- and post-insemination (i.e., total reproductive success) and during
167 post-insemination alone using a novel male competitor (Fig 2B). Total reproductive success was
168 slightly, though significantly, poorer than the null expectation of equal competitive ability
169 between ancestral male and competitor male backgrounds (proportions test: $\chi^2 = 6.87$, d.f. = 1, p
170 < 0.01 , 95% C.I. of ancestral competitive success = 40.4–48.6%). Ancestral male sperm
171 competitive ability was especially poor with an average of 4.1% of progeny coming from

172 ancestral males relative to the competitor (proportions test: $\chi^2 = 863$, d.f. = 1, $p < 0.0001$, 95%
173 C.I. of ancestral sperm competitive success = 3.0–5.5%). Therefore, in the ancestral population
174 post-insemination success only contributed 9.2% to the overall reproductive success of males
175 (Fig 2C). The poor reproductive success of ancestral males under competitive conditions
176 indicates the opportunity for selection – particularly gametic selection – to improve male
177 competitive ability was high.

178 **Post-insemination selection drove evolutionary change in males**

179 We quantified total reproductive success for each replicate population after 10 selective events
180 occurring over 30 generations of evolution under the same highly competitive conditions used to
181 assay the ancestral males. The contribution of post-insemination increased across all evolved
182 replicates relative to the ancestor, such that on average post-insemination success contributed
183 26.7% to 34.7% of total male reproductive success (Fig 2C). The BS-P&P and WS-PO regimes
184 trended towards a higher fraction of total reproductive success that could be attributed to post-
185 insemination success across replicate means, suggesting that enhanced post-insemination
186 competition positively affects fertilization success. Interestingly, post-insemination contribution
187 increased to 79.7% in a single BS-P&P replicate. This evolutionary increase was due to a 13-fold
188 increase in post-insemination success and only a 1.4-fold increase in total reproductive success.

189 Overall, the increased contribution of post-insemination dynamics was driven by the
190 significant increase in post-insemination reproductive success of evolved males compared to
191 ancestral males (Fig 2D; WS-P&P: z -value = 3.7, $p < 0.001$; BS-P&P: z -value = 3.6, $p = 0.001$;
192 WS-PO: z -value = 3.4, $p = 0.002$; BS-PO: z -value = 4.0, $p < 0.001$). Once again, the BS-PO
193 regime showed the strongest evolutionary response with a 6.8-fold increase from the ancestor,
194 which supports the hypothesis that enhanced post-insemination competition increases the
195 efficacy of sexual selection. Additionally, the WS-PO regime – the regime with the lowest levels
196 of post-insemination competition – comparatively showed the lowest mean evolutionary change
197 from the ancestor, though overall the evolutionary response was still strong. However, a post hoc
198 test to determine if experimental evolution under directed sexual selection increased the rate at
199 which post-insemination evolved relative to the WS-P&P baseline conditions showed no
200 significant difference between regimes, suggesting a strong underlying selective pressure on
201 sperm competitive ability.

202 Total reproductive success of evolved males compared to ancestral males also increased
203 significantly across regimes (WS-P&P: z-value = 4.7, $p < 0.001$; BS-P&P: z-value = 2.7, $p =$
204 0.02; WS-PO: z-value = 3.5, $p < 0.001$; BS-PO: z-value = 3.6, $p < 0.001$), though to a lesser
205 extent than post-insemination success alone (Fig 2D). Interestingly, only the BS-P&P regime
206 showed a significant effect of sexual selection ($z = -3.6$, $p < 0.001$) compared to the baseline
207 WS-P&P regime. Contrary to expectation [5,28], enhanced pre-insemination competition
208 reduced the evolutionary response in male reproductive success. The WS-PO and BS-PO were
209 not significantly different from the baseline. Thus, increasing the opportunity for pre-
210 insemination sexual selection did not lead to faster evolution. Rather, enhanced pre-insemination
211 competition appeared to hinder the rate of evolution of male reproductive success.

212 **Effective population size reflects strong selection**

213 The effective population size (N_e) ranged from 16% to 24% of the census size ($N = 5,000$) across all
214 replicates and regimes (Fig S3; File S3). Regimes where post-insemination interactions were
215 isolated had on average lower effective population sizes across all chromosomes than the WS-
216 P&P and BS-P&P regimes. However, there was no significant effect of regime on N_e (ANOVA:
217 $F = 0.72$, d.f. = 3, $p = 0.54$). Variance in reproductive success impacts N_e , especially when the
218 sex ratio of breeding individuals is skewed. We calculated the upper bound on the number of
219 breeding males [29], under the assumption that all females reproduced and the reduction in
220 population size was due to variance in male reproductive success alone. For the estimated N_e
221 range, this analysis suggests that only 222-333 males reproduced (8.9-13.3% of the census male
222 population), supporting strong sexual selection acted on males.

223 Given the XX/XO chromosomal sex determination system of *C. elegans*, we expected the
224 estimated effective population size of the X chromosome to be approximately 75% of the
225 estimated effective population size of the autosomes. The effective population size was
226 significantly different between the autosomes and sex chromosome ($t = 3.34$, d.f. = 24.5, $p <$
227 0.01). However, contrary to expectation, the mean effective population size estimated using X
228 chromosome SNPs was 1.9 times larger than that estimated using autosomal SNPs.

229 **Sperm competitive ability is a polygenic trait**

230 We fit two complementary models to determine if the frequency of alleles at each SNP changed
231 from the ancestral population to the evolved population in each regime. Model 1 used a post hoc

232 approach to compare SNP counts in the evolved and ancestral populations (Model 1: $\text{glm}(\text{SNP} \sim$
233 regime), linear hypothesis test: $\text{Anc} - \text{Evolved}_{\text{regime}} = 0$) and identified 3,461 significant SNPs
234 after a Bonferroni correction ($p < 7.43e-6$). The significance trends of Model 1 (File S4) support
235 the more robust findings of Model 2 (File S5). Here we fit independent models for each regime
236 that included sampling at two intermediate generations (Model 2: $\text{glm}(\text{SNP}_{\text{regime}} \sim \text{time})$). In
237 Model 2, we identified 160 non-overlapping significance peaks across the five autosomes and the
238 X chromosome, indicating that male reproductive success is polygenic (Fig 3, File S6).
239 Significance peaks showed a strong chromosome arm-center structure, likely driven by the
240 higher density of SNPs on the chromosome arms (Fig S2). Thirty-one peaks were shared across
241 all regimes (Fig 3, Fig S4). The BS-PO regime had the highest number of significant SNPs ($n =$
242 1,994) as well as the highest number of unique significance peaks ($n = 32$). The WS-PO regime
243 and the shared WS-PO and BS-PO regimes represent the third and fourth highest groupings,
244 reinforcing that isolated gametic sexual selection resulted in a strong polygenic genomic
245 response (Fig S4). The WS-P&P regime had the fewest number of significance peaks and only
246 three peaks were unique to this regime.

247 Linkage disequilibrium was low between SNPs and significance peaks could be narrowed
248 down to small genomic regions (File S6). The median peak width was 362.5 base pairs. The
249 largest peak spanned a 10,753 base pair region on the right arm of Chromosome I and lies in the
250 intron of gene C17H1.2 (Fig S5). This gene exhibits male-biased expression, though its function
251 is uncharacterized [30]. The majority of significance peaks ($n = 108$) fell within a genic region,
252 while 26 peaks were intergenic (File S6). Twenty-three peaks were located in pseudogenes and
253 an additional three peaks overlapped with coding genes and pseudogenes.

254 To determine the functional pathways underlying improved male reproductive success,
255 we examined the gene ontology (GO) terms associated with the genes underlying significance
256 peaks (Fig S6; File S6). The most common molecular function identified was SCF ubiquitin
257 ligase complex formation through F-box proteins ($n = 16$). Several genes were also related to
258 each carbohydrate binding, G-coupled protein receptor activity, and transferase transporter
259 activity. Six genes were associated with some form of RNA. However, 47.5% of genes were
260 uncharacterized in function, identifying a lack of male-specific functional knowledge.

261

262 Discussion

263 Quantifying the balance of pre- and post-insemination selection is critical for understanding how
264 male reproductive fitness is comprised and how reproductive success evolves. This knowledge
265 translates to better understanding how sexual selection contributes to population adaptation. We
266 took a direct approach to isolate post-insemination from pre-insemination dynamics by coupling
267 transgenic induction systems within an experimental evolution framework to examine whether
268 these reproductive phases contribute in an additive or antagonistic manner to male reproductive
269 fitness. All treatments showed a strong, rapid response to selection at both the phenotypic and
270 genomic levels (Fig 2 and 3). Phenotypic results indicate that post-insemination selection was the
271 major driver of male evolution. Genomic results support the importance of post-insemination
272 selection and suggest that selection during this phase increased the efficacy of selection.
273 Additionally, reproductive success is a highly polygenic trait with genes on all chromosomes
274 contributing to the response to selection. These results provide new insights on the complexity of
275 post-insemination dynamics and highlight the importance of considering all phases of
276 reproduction.

277 The balance between pre- and post-insemination selection was complex and depended on
278 the strength of selection imposed. At the phenotypic level, the within-strain competition
279 treatments suggest that pre- and post-insemination act in an additive manner to increase male
280 reproductive fitness (Fig 2). However, this pattern does not hold under enhanced between-strain
281 competitive conditions. Instead, contrary to expectation, increased male-male competition (BS-
282 P&P) decreased the rate of adaptation relative to base levels (WS-P&P). These increased
283 competitive interactions could potentially harm females as a byproduct (i.e., sexual conflict) and
284 therefore reduce female reproductive rate. However, the BS-PO treatment had the same number
285 of males attempting to mate with females as the BS-P&P, the difference being that the BS-PO
286 males could not transfer sperm post-mating. Thus, the increased number of males actually
287 inseminating females is likely the contributing source of the decreased evolutionary response.
288 While it seems possible that increased competition among sperm led to the decrease in fecundity
289 [31], it is also possible that females altered egg-laying rates in response to the amount of sperm
290 present as a result of a resource trade-off between reproductive and maintenance functions. To
291 our knowledge, no studies have quantified this relationship in nematodes.

292 In contrast, increased sperm competition appeared to improve the rate of adaptation in
293 males. BS-PO males trended towards the highest rate of increase in post-insemination success

294 and post-insemination contributed the most to their overall reproductive response. While these
295 comparative trends were not significant at the phenotypic level, at the genomic level populations
296 evolved under increased sperm competition had the strongest genomic response across dozens of
297 genes (Fig 3 and S4). Interestingly, populations evolved under reduced sperm competitive
298 dynamics (WS-PO) also showed a strong genomic response, suggesting that isolating post-
299 insemination dynamics from pre-insemination dynamics allowed sexual selection to act more
300 efficiently. While we isolated post-insemination through transgenic induction, this type of effect
301 could be seen in nature if females were to mate with males over distinct periods of time and store
302 sperm for later use.

303 Our method of population construction generated little haplotype structure, which
304 allowed us to map genetic elements that responded to selection with high precision. A challenge
305 in many quantitative trait loci [32] and evolve-and-resequence studies [33] is narrowing down
306 the regions of selection to make specific statements on the genetic architecture of traits. In
307 contrast, here we have high confidence that reproductive success and sperm competitive success
308 are complex traits underlaid by over 60 genes (Fig 3 and S4). In most cases, we were able to
309 narrow the region under selection to just a few hundred base pairs. While this precision should in
310 principle allow us to identify the causal basis of the genetic response, given the highly polygenic
311 structure of these complex traits, each contributing gene likely contributes a small effect, which
312 makes the next step of functional molecular characterization challenging. To help prioritize this
313 process, we performed a GO analysis to look for patterns in molecular functions or biological
314 processes (Fig S6). F-box proteins involved in protein-protein interactions, such as ubiquitin-
315 ligase complex formation [34], showed a strong response in all treatments. Though their exact
316 function is unknown, many of the several hundred *C. elegans* F-box genes show signatures of
317 positive selection in wild isolates, suggesting that selective conditions observed in nature were
318 mimicked in the lab [35]. However, nearly half of the identified genes were uncharacterized in
319 function, despite *C. elegans* being a major model system. These genes represent a candidate list
320 for future molecular studies to characterize the networks underlying male reproductive function.
321 In particular, gene C17H1.2 is of interest for future study as it has a large significance peak
322 falling within the second intron and exhibits male-biased expression patterns.

323 Sexual selection has a large effect on population size by limiting the number of
324 successfully breeding adults [reviewed in 36]. We estimated the effective population size to be

325 less than one quarter of the enforced census size. If one assumes that nearly all females are mated
326 as an upper bound, this difference suggests that on average approximately 10% of males sired all
327 offspring (Fig S3). This is the very definition of opportunity for sexual selection [7] and is
328 consistent with our conclusion that strong sexual selection acted on these populations even in the
329 base level treatment (WS-P&P). Interestingly, the effective population size of the X chromosome
330 was larger than expected given the XX/XO sex determination system of *Caenorhabditis*
331 nematodes, which would suggest that the effective population size of the X chromosome should
332 be 3/4 that of the autosomes under neutral expectations. The flip in the N_e ratio between the X
333 and autosomes is further evidence that the response to selection is driven by sexual interactions
334 among males, as the X chromosome is in males 1/3 of the time while autosomes are in males 1/2
335 the time, and so the autosomes are more susceptible to drift induced by variance in mating
336 success specially among males [36,37]. Interestingly, the X chromosome also had the fewest
337 number of significance peaks, so in addition to the demography of the X chromosome itself, it is
338 also possible that there may be additional reductions in autosomal variation due hitchhiking [36].

339 Darwin first noted that the existence of elaborate sex-specific traits seemed at odds with
340 regular evolutionary processes, and more than a hundred of years of research has subsequently
341 focused on understanding how sexual selection drives diversity for these traits within and
342 between populations. Our work indicates that the cryptic phenotypes and molecular effects that
343 emerge during post-insemination interactions are equally important in determining fertilization
344 success and likely to be just as genetically complex.

345

346 **Materials and methods**

347 **Molecular biology**

348 Guides targeting sequences in the same intergenic regions utilized by the ttTi4348 and ttTi5605
349 MosSCI sites have been previously described [19,38]. Additional guide sequences were chosen
350 using the Benchling CRISPR design tool, based on the models of Doench *et al.* [39] and Hsu *et*
351 *al.* [40], and the Sequence Scan for CRISPR tool [41]. Guides were inserted into pDD162
352 (Addgene #47549) [42] using the Q5 site-directed mutagenesis kit (NEB) or ordered as
353 cr:tracrRNAs from Synthego. A complete list of guide sequences can be found in Table S1.

354 Repair template plasmids were assembled using the NEBuilder HiFI Kit (NEB) from a
355 combination of restriction digest fragments and PCR products. PCR products were generated
356 using the 2x Q5 PCR Master Mix (NEB) in accordance with manufacturer instructions. Details
357 of plasmid construction can be found in the supplemental methods and Tables S2 and S3.
358 Plasmids were purified using the ZR Plasmid Miniprep kit (Zymo) and all plasmid assembly
359 junctions were confirmed by Sanger sequencing.

360 **Strain generation**

361 All strains used in this study are listed in Table S4 and depicted schematically in Figure S1.
362 Insertion of transgenes was done by CRISPR/Cas9 using standard methods. Briefly, a mixture of
363 10ng/μl repair template plasmid, 50ng/μl plasmid encoding CAS9 and the guide RNA and
364 2.5ng/μl pCFJ421 (Addgene #34876) [43] was injected into the gonad of young adult
365 hermaphrodites. Where hygromycin resistance (HygR) was used as a selectable event, two to
366 three days after injection, hygromycin B (A.G. Scientific, Inc.) was added to the plates at a final
367 concentration of 250μg/ml. Successful insertion was confirmed by PCR and Sanger sequencing.

368 To generate the male sterility induction strain PX624, *pie-1p::TIR-1* was inserted into the
369 Chromosome I site and a degron tag was added to the native *spe-44* locus of JU2526 as in
370 Kasimatis *et al.* [19] (Fig S1A, C). The majority of exons 2-4 of the native *fog-2* gene were then
371 deleted using the guides and oligonucleotide repair template listed in Table S1 and Table S3.
372 Microinjections and *dpy-10* co-marker screening were done as previously described [19,44]. This
373 strain represents the predecessor for the experimental evolution ancestral population (see
374 “Generating genetic diversity”).

375 The *hsp-16.41p::PEEL-1 + rpl-28p::mKate2 + rps-0p::HygR* three gene cassette was
376 inserted into the Chromosome I site of CB4856. Individuals with confirmed inserts were crossed
377 to JK574, containing *fog-2(q71)*, and backcrossed 4 times to CB4856 (Fig S1B). A single pair
378 was then chosen for 14 generations of inbreeding to create strain PX626. To introduce a second
379 copy of *hsp-16.41p::PEEL-1*, a *hsp-16.41p::PEEL-1 + loxP::rps-0p::HygR::loxP* two gene
380 cassette was inserted into the Chromosome II site (Fig S1). The HygR gene was then removed by
381 injection of a CRE expressing plasmid pZCS23 [45] at 10ng/μl, with removal monitored by

382 PCR, to generate PX630. PX626 was crossed to PX630 to generate the final novel, bioassay
383 competitor strain PX631 (Fig S1E).

384 To generate a lethality and male sterility induction strain, PX624 was crossed with
385 PX631 and then backcrossed 5 times with PX624 to introgress *hsp-16.41p::PEEL-1* in the
386 Chromosome II site to create strain PX655. Since the Chromosome I site of PX624 is occupied
387 by *pie-1p::TIR-1*, CRISPR/Cas9 was used to insert the *hsp-16.41p::PEEL-1 + rpl-28p::mKate2*
388 + *rps-0p::HygR* three gene cassette into PX624 at a site on Chromosome III between *nac-3* and
389 K08E5.5 that has not been previously used for transgene insertion, creating PX656. PX655 and
390 PX656 were then crossed to create the final competitor strain PX658 (Fig S1D).

391 **Generating genetic diversity**

392 The male sterility induction strain (PX624) was exposed to ethyl methanesulfonate (EMS) to
393 induce genetic variation (Fig S1). Populations of 8,000-10,000 age-synchronized L4 worms were
394 divided into 4 technical replicates and suspended in M9 buffer. Worms were incubated in 12.5
395 mM EMS for 4 hours at 20°C, after which they were rinsed in M9 buffer and plated on NGM-
396 agar plates. Replicate populations were given two recovery and growth generations with ample
397 food following a mutagenesis event. A total of five low-dose mutagenesis rounds coupled with
398 recovery generations were performed. During each of the recovery rounds, a subset of worms
399 from each replicate were screened on NGM-agar plates containing 1 mM indole-3-acetic acid
400 (Auxin, Alfa Aesar) following Kasimatis *et al.* [19] to test if mutagenesis had compromised the
401 integrity of the sterility induction system. Specifically, if eggs were observed on an auxin-
402 containing plate, then that replicate was removed and another replicate was subdivided, so a total
403 of four replicate populations were always maintained.

404 After the final round of mutagenesis and recovery, replicate populations were maintained
405 for five generations of lab adaptation. They were then combined for an additional 10 generations
406 of lab adaptation with a population size of approximately 30,000 worms. The integrity of the
407 sterility induction system continued to be screened every two generations throughout the entire

408 lab adaptation process. This genetically diverse, male sterility induction strain PX632 represents
409 the ancestral experimental evolution population (Fig S1).

410 **Experimental design and worm culture**

411 The ancestral population (PX632) was divided into four experimental regimes, which varied
412 based on total (i.e., pre- and post-insemination) or sperm (i.e., post-insemination) competition
413 dynamics occurring either within the evolving strain alone or between the evolving strain and
414 competitor strain (PX658): within-strain pre- and post-insemination competition (WS-P&P),
415 within-strain post-insemination only competition (WS-PO), between-strain pre- and post-
416 insemination competition (BS-P&P), and between-strain post-insemination only competition
417 (BS-PO).

418 Each regime had six replicate populations ~~and experimentally~~ evolved for 30 generations.
419 Ten selective events occurred over the course of experimental evolution denoted by the induction
420 of sterility, the addition of competitors, and the induction of sterility and addition of competitors
421 in the WS-PO, BS-P&P, and BS-PO regimes, respectively (Fig 1 & Fig 2A). The WS-P&P had
422 no direct selection applied. Each selective event was followed by a recovery generation, where
423 no direct selection was applied, to allow the populations to return to the census size. During the
424 recovery generation, a subset of worms from the regimes with sterility induction were screened
425 on auxin-containing plates to ensure the sterility induction system was functional. Additionally, a
426 subset of worms from all replicates was frozen for future stocks. The detailed selection
427 procedure follows.

428 To start each selective event age synchronized L1 worms were plated onto five 10 cm
429 NGM-agar plates seeded with OP50 *Escherichia coli* at 20°C with a density of 1,000 worms per
430 plate, giving a census size of 5,000 worms per replicate per regime [46,47]. Forty-eight hours
431 later, experimental regimes with sterility induction (WS-PO and BS-PO) were transferred to
432 NGM-agar plates containing 1mM auxin. Experimental regimes without sterility induction (WS-
433 P&P and BS-P&P) were transferred to fresh NGM-agar plates. For all transfers, worms within a
434 replicate were pooled and then redistributed across five plates with a density of 1,000 worms per
435 plate. After 24 hours, males from the competitor strain PX658 were filter-separated from females
436 using a 35 um Nitex nylon filter and added to experimental regimes with competition at a mean
437 density of 200 competitor males per plate (evolving to competitor ratio of 1:2.5). After another
438 24 hours, eggs were collected from all replicates, hatched, and age synchronized. To ensure that

439 only progeny from the evolving males and not from the competitor males were being propagated,
440 larval lethality of competitor progeny was induced following Seidel *et al.* [22]. Briefly,
441 approximately 5,000 L3 worms were suspended in 5 mL of S-Basal and heat-shocked in a 35°C
442 sealed water bath for 2.5 hours to activate ectopic expression of the lethal protein PEEL-1. After
443 heat-shock, worms were plated on NGM-agar plates to end the selective event. All experimental
444 regimes were subjected to the heat-shock procedure, even if competitor worms were not added.

445 A subset of approximately 200 worms from the competition and sterility and competition
446 regimes were removed prior to heat-shock and fluorescence screened to determine the proportion
447 of progeny coming from the competitor worms, which expressed red fluorescent protein (RFP),
448 versus the evolving worms, which had no fluorescence.

449 The competitor strain PX658 was maintained on NGM-agar plates seeded with OP50 *E.*
450 *coli* at 20°C in population sizes of approximately 20,000 worms. The competitor strain was reset
451 from freezer stocks every 3 weeks (~4 generations) to prevent adaptation and maintain a constant
452 competitive phenotype.

453 **Fertility assays**

454 We assayed the fertility of the ancestor and all the evolved replicates (N = 13 populations) to
455 determine the total competitive reproductive success of males as well as their sperm competitive
456 success. The assay conditions mimicked the environment under which worms evolve. Total
457 competitive reproductive success was assessed by adding the novel competitor PX631 in equal
458 proportion to evolving males. Sperm competitive success was assessed by inducing sterility of
459 the evolving male before adding the novel competitor in equal proportion to evolving males. The
460 use of the novel competitor and high competition ratio acted as a “stress-test” of male
461 competitive ability. Both assays were performed with a population of 250 evolving females, 250
462 evolving males, and 250 novel competitors. After a 24-hour competition period, eggs were
463 collected, hatched, and age synchronized for screening. At least 200 L3 progeny were counted
464 for each assay and then fluorescence-screened for the proportion of progeny coming from
465 evolving (RFP minus) or competitor (RFP plus) males. Three independent biological replicates
466 were done for each assay across all experimental evolution replicates (File S7).

467 Fertility data were analyzed using the R statistical language v4.0.0 [48]. An equality of
468 proportions test was performed on the ancestral data to determine if ancestral males sired half the
469 total progeny under total competitive and sperm competitive conditions. The evolved male

470 fertility data were analyzed using a linear model (GLM) framework with random effects using
471 the *lme4* v.1.13 package [49]. The *multcomp* package [50] was then used to perform a planned
472 comparisons tests with defined contrasts to determine if: i) evolutionary change from the
473 ancestral population occurred, and ii) experimental evolution under direct sexual selection
474 affected reproductive success differently than baseline selection alone (i.e., WS-P&P).

475 **Genome sequencing, mapping, and SNP calling**

476 We performed whole-genome sequencing on pooled samples of 2,000-3,000 L1 worms from
477 generations 0, 13, 22, and 31. Three independent pooled extractions were done for the ancestral
478 population (i.e., generation 0) to capture as many segregating variants as possible. Worms were
479 flash frozen and DNA was isolated using Genomic DNA Clean and Concentrator-10 (Zymo).
480 Libraries were prepared using the Nextera DNA Sample Prep kit (Illumina) starting from 5 ng of
481 DNA. 100 bp paired-end reads were sequenced on an Illumina HiSeq 4000 at the University of
482 Oregon Genomics and Cell Characterization Core Facility (Eugene, OR). The average genome-
483 wide sequencing coverage for generations 0, 13, 22, and 31 was 162×, 24×, 26×, 50×,
484 respectively.

485 Reads were trimmed using skewer v0.2.2 [51] to remove low quality bases (parameters: -
486 x CTGTCTCTTATA -t 12 -l 30 -r 0.01 -d 0.01 -q 20). The trimmed reads were mapped to the *C.*
487 *elegans* N2 reference genome (PRJNA13758-WS274) [30] using BWA-MEM v0.7.17
488 (parameters: -t 8 -M) [52] and then sorted using SAMtools v1.5 [53]. We removed PCR
489 duplicates with MarkDuplicates in Picard v2.6.0 (<https://github.com/broadinstitute/picard>),
490 realigned insertions/deletions with IndelRealigner in GATK v3.7
491 (<https://github.com/broadinstitute/gatk/#authors>), and called variants with mpileup in bcftools
492 v1.5 [54]. The mpileup file was then converted to a genotype-called vcf file, insertions/deletions
493 were removed, and the allelic depth was extracted for all biallelic SNPs for further analysis.

494 To improve the reliability of the analysis pipeline, additional filtering was done using R
495 [48]. Repeat regions were masked based the *C. elegans* N2 reference
496 (<https://gist.github.com/danielecook/cfaa5c359d99bcad3200>) and SNPs in the upper and lower
497 5% tails of the total coverage distribution (i.e., >342× and ≤20×, respectively) were removed.
498 This yielded a total of 326,648 SNPs to be considered for analyses.

499 **Estimation and candidate SNP inference**

500 Genetic diversity summary statistics were estimated for the ancestral population from 32,299
501 SNPs. Coverage-weighted average heterozygosity (π) was calculated following Begun et al. [55].
502 SNP density (θ_w) was calculated across 1kb sliding windows. We performed a Kolmogorov-
503 Smirnov test to determine if the site frequency spectrum, π , and θ_w differed between
504 chromosome arm domains and center domains [25]. Effective population size (N_e) was
505 calculated per chromosome for each of the evolved regime replicates following Waples [56] Plan
506 II sampling [57]. An analysis of variance was performed in R to determine if the genome-wide
507 N_e differed between regimes and Welch's Two-Sample t-test was performed to determine if the
508 estimated N_e on autosomes differed from the X chromosome. We estimated the upper bound on
509 the number of breeding males (N_m) by solving the equation $N_e = (4 N_m N_f) / (N_m + N_f)$ for N_m
510 using the estimated effective population sizes and assuming that all females reproduced ($N_f =$
511 2,500).

512 Allele count data were analyzed using R [48] following two complementary models.
513 Model 1 fit allele counts for ancestral and evolved populations using a generalized linear mixed
514 model with a binomial logistic distribution: $\text{glm}(\text{SNP} \sim \text{regime})$. The SNP data going into Model
515 1 were filtered to ensure each SNP was present in the ancestor and at least ten of the evolved
516 replicates. A total of 263,373 SNPs fit the full model (File S4). The *multcomp* package [50] was
517 then used to perform a planned comparisons tests with defined contrasts to determine if
518 experimental evolution under direct sexual selection affects the genome differently than baseline
519 selection alone (i.e., WS-P&P). Model 2 fit allele counts across all time points for each regime
520 separately, again using a generalized linear mixed model with a binomial logistic distribution:
521 $\text{glm}(\text{SNP}_{\text{regime}} \sim \text{time})$. The SNP data going into Model 2 were filtered to ensure each SNP was
522 present in the ancestor and at least nine occurrences across replicates and time points. A total of
523 202,926 SNPs, 222,731 SNPs, 200,324 SNPs, and 204,946 SNPs fit the full model for the WS-
524 P&P, WS-PO, BS-P&P, and BS-PO regimes, respectively (File S5). For both models,
525 significance was determined using a genome-wide Bonferroni cut-off.

526 A significance peak was called if five or more significant SNPs fell in a 1kb window.
527 Peaks were classified as occurring within a gene (intragenic) or between genes (intergenic) using
528 JBrowse in WormBase [30]. If multiple 1kb windows fell within a single gene, then the windows
529 were combined and called as a single intragenic peak. The molecular and biological functions of

530 the associated genes were determined using gene ontology analysis in UniProt [58] and
531 QuickGO [59].

532 **Data accessibility**

533 The oligonucleotides and synthetic constructs used in this study are available as Supplemental
534 Tables S1-S3. The sequence data will be made publicly available on NCBI prior to publication.
535 Model summary statistics for the genomic analyses (Files S1-S6) and the fertility data (File S7)
536 are available in the Figshare repository <https://figshare.com/s/735e8011f9a1239a5c85>, which
537 will be made public upon acceptance.. All R scripts are available via the GitHub repository
538 https://github.com/katjakasimatis/postinsemination_expevol. Worm strains PX624, PX631, and
539 PX658 will be made available from the *Caenorhabditis* Genetics Center. All other strains are
540 available from the Phillips Lab upon request.

541

542

543

544 **Acknowledgements**

545 We thank Brennen Jamison, Erik Johnson, and Christine Sedore for assistance during
546 experimental evolution and Anastasia Teterina for advice on the genomic analyses. We thank
547 Levi Morran, Bill Rice, Locke Rowe, and the Phillips lab for their helpful discussion. This work
548 was conducted in part using the resources of the University of Oregon Genomics and Cell
549 Characterization Core Facility and Research Advanced Computing Services.

550

551

552 **Funding**

553 This work was funded by National Institutes of Health grant R35GM131838 to PCP. KRK is
554 supported by a Natural Sciences and Engineering Research Council of Canada Banting
555 Postdoctoral Fellowship. The funders had no role in study design, data collection and analysis,
556 decision to publish, or preparation of the manuscript.

557

558

559 **Author contributions**

560 KRK and PCP devised the project. KRK and MJMS created the strains. KRK collected the
561 experimental evolution data with assistance from RL and AS. JHW prepared the genomic
562 libraries. KRK analyzed the data. KRK and PCP wrote the manuscript with the support of the
563 other authors.

564

565

566 **References**

- 567 1. Andersson M. *Sexual Selection*. New York: Princeton University Press; 1994.
- 568 2. Lewontin R. The units of selection. *Annu Rev Ecol Syst.* 1970;1: 1–18.
- 569 3. Immler S, Otto SP. The Evolutionary Consequences of Selection at the Haploid Gametic
570 Stage. *Am Nat.* 2018;192: 241–249.
- 571 4. Lorch PD, Stephen Proulx, Rowe L, Day T. Condition-dependent sexual selection can
572 accelerate adaptation. *Evol Ecol Res.* 2003;5: 867–881.
- 573 5. Candolin U, Heuschele J. Is sexual selection beneficial during adaptation to environmental
574 change? *Trends Ecol Evol.* 2008;23: 446–452.
- 575 6. Lande R. Models of speciation by sexual selection on polygenic traits. *Proc Natl Acad Sci*
576 *USA.* 1981;78: 3721–3725.
- 577 7. Arnold SJ, Wade MJ. On the measurement of natural and sexual selection: theory.
578 *Evolution.* 1984;38: 709–719.
- 579 8. Evans JP, Garcia-Gonzalez F. The total opportunity for sexual selection and the
580 integration of pre- and post-mating episodes of sexual selection in a complex world. *J*
581 *Evol Biol.* 2016;29: 2338–2361.
- 582 9. Pischedda A, Rice WR. Partitioning sexual selection into its mating success and
583 fertilization success components. *Proc Natl Acad Sci USA.* 2012;109: 2049–2053.
- 584 10. Rose E, Paczolt KA, Jones AG. The contributions of premating and postmating selection
585 episodes to total selection in sex-role-reversed Gulf pipefish. *Am Nat.* 2013;182: 410–420.
- 586 11. Marie-Orleach L, Janicke T, Vizoso DB, David P, Schärer L. Quantifying episodes of
587 sexual selection: Insights from a transparent worm with fluorescent sperm. *Evolution.*
588 2016;70: 314–328.

- 589 12. Devigili A, Evans JP, Di Nisio A, Pilastro A. Multivariate selection drives concordant
590 patterns of pre- and postcopulatory sexual selection in a livebearing fish. *Nat Commun.*
591 2015;6: 1–9.
- 592 13. Collet J, Richardson DS, Worley K, Pizzari T. Sexual selection and the differential effect
593 of polyandry. *Proc Natl Acad Sci USA.* 2012;109: 8641–8645.
- 594 14. Turnell BR, Shaw KL. High opportunity for postcopulatory sexual selection under field
595 conditions. *Evolution.* 2015;69: 2094–2104.
- 596 15. Pélissié B, Jarne P, Sarda V, David P. Disentangling precopulatory and postcopulatory
597 sexual selection in polyandrous species. *Evolution.* 2014;68: 1320–1331.
- 598 16. Begun DJ, Whitley P, Todd BL, Waldrip-Dail HM, Clark AG. Molecular population
599 genetics of male accessory gland proteins in *Drosophila*. *Genetics.* 2000;156: 1879–1888.
- 600 17. Swanson WJ, Vacquier VD. Reproductive Protein Evolution. *Annu Rev Ecol Syst.*
601 2002;33: 161–179.
- 602 18. Stewart AD, Phillips PC. Selection and maintenance of androdioecy in *Caenorhabditis*
603 *elegans*. *Genetics.* 2002;160: 975–982.
- 604 19. Kasimatis KR, Moerdyk-Schauwecker MJ, Phillips PC. Auxin-mediated sterility
605 induction system for longevity and mating studies in *Caenorhabditis elegans*. *G3.* 2018;8:
606 2655–2662.
- 607 20. Schlötterer C, Kofler R, Versace E, Tobler R, Franssen SU. Combining experimental
608 evolution with next-generation sequencing: a powerful tool to study adaptation from
609 standing genetic variation. *Heredity.* 2015;114: 431–440.
- 610 21. Teotonio H, Estes S, Phillips PC, Baer CF. Experimental Evolution with *Caenorhabditis*
611 *Nematodes*. *Genetics.* 2017;206: 691–716.
- 612 22. Seidel HS, Ailion M, Li J, van Oudenaarden A, Rockman MV, Kruglyak L. A novel
613 sperm-delivered toxin causes late-stage embryo lethality and transmission ratio distortion
614 in *C. elegans*. *PLoS Biol.* 2011;9: e1001115–21.
- 615 23. Gengyo-Ando K, Mitani S. Characterization of mutations induced by ethyl
616 methanesulfonate, UV, and trimethylpsoralen in the nematode *Caenorhabditis elegans*.
617 *Biochem Biophys Res Commun.* 2000;269: 64–69.
- 618 24. Cutter AD, Baird SE, Charlesworth D. High nucleotide polymorphism and rapid decay of
619 linkage disequilibrium in wild populations of *Caenorhabditis remanei*. *Genetics.*
620 2006;174: 901–913.
- 621 25. Rockman MV, Kruglyak L. Recombinational Landscape and Population Genomics of
622 *Caenorhabditis elegans*. *PLoS Genetics.* 2009;5: e1000419–16.

- 623 26. Lee D, Zdraljevic S, Stevens L, Wang Y, Tanny RE, Crombie TA, et al. Balancing
624 selection maintains ancient genetic diversity in *C. elegans*. bioRxiv. 2020: 1–41.
625 doi:10.1101/2020.07.23.218420
- 626 27. Andersen EC, Gerke JP, Shapiro JA, Crissman JR, Ghosh R, Bloom JS, et al.
627 Chromosome-scale selective sweeps shape *Caenorhabditis elegans* genomic diversity. Nat
628 Rev Genet. 2012;44: 285–290.
- 629 28. Lande R. Sexual dimorphism, sexual selection, and adaptation in polygenic characters.
630 Evol. 1980;34: 292–305.
- 631 29. Crow JF, Kimura M. An introduction to population genetics theory. New York: Harper
632 and Rowe; 1970.
- 633 30. Harris TW, Arnaboldi V, Cain S, Chan J, Chen WJ, Cho J, et al. WormBase: a modern
634 Model Organism Information Resource. Nucleic Acids Res. 2019;gkz920.
- 635 31. Holland B, Rice WR. Experimental removal of sexual selection reverses intersexual
636 antagonistic coevolution and removes a reproductive load. Proc Natl Acad Sci USA.
637 1999;96: 5083–5088.
- 638 32. Mackay TFC, Stone EA, Ayroles JF. The genetics of quantitative traits: challenges and
639 prospects. Nat Rev Genet. 2009;10: 565–577.
- 640 33. Otte KA, Nolte V, Mallard F, Schlötterer C. The adaptive architecture is shaped by
641 population ancestry and not by selection regime. bioRxiv. 2020;1–38.
642 doi:10.1101/2020.06.25.170878
- 643 34. Kipreos ET, Pagano M. The F-box protein family. Genome Biol. 2000;1: 3002.1–3002.7.
- 644 35. Ma F, Lau CY, Zheng C. Large genetic diversity and strong positive selection in F-box
645 and GPCR genes among the wild isolates of *Caenorhabditis elegans*. Genome Biol Evol.
646 2021;13: evab048.
- 647 36. Charlesworth B. Fundamental concepts in genetics: effective population size and patterns
648 of molecular evolution and variation. Nat Rev Genet. 2009;10: 195–205.
- 649 37. Corl A, Ellegren H. The genomic signature of sexual selection in the genetic diversity of
650 the sex chromosomes and autosomes. Evol. 2012;66: 2138–2149.
- 651 38. Dickinson DJ, Pani AM, Heppert JK, Higgins CD, 2015. Streamlined genome engineering
652 with a self-excising drug selection cassette. Genetics. 2015;200: 1035–1049.
- 653 39. Doench JG, Fusi N, Sullender M, Hegde M, Vaimberg EW, Donovan KF, et al. Optimized
654 sgRNA design to maximize activity and minimize off-target effects of CRISPR-Cas9. Nat
655 Biotechnol 2016 34:3. 2016;34: 184–191.

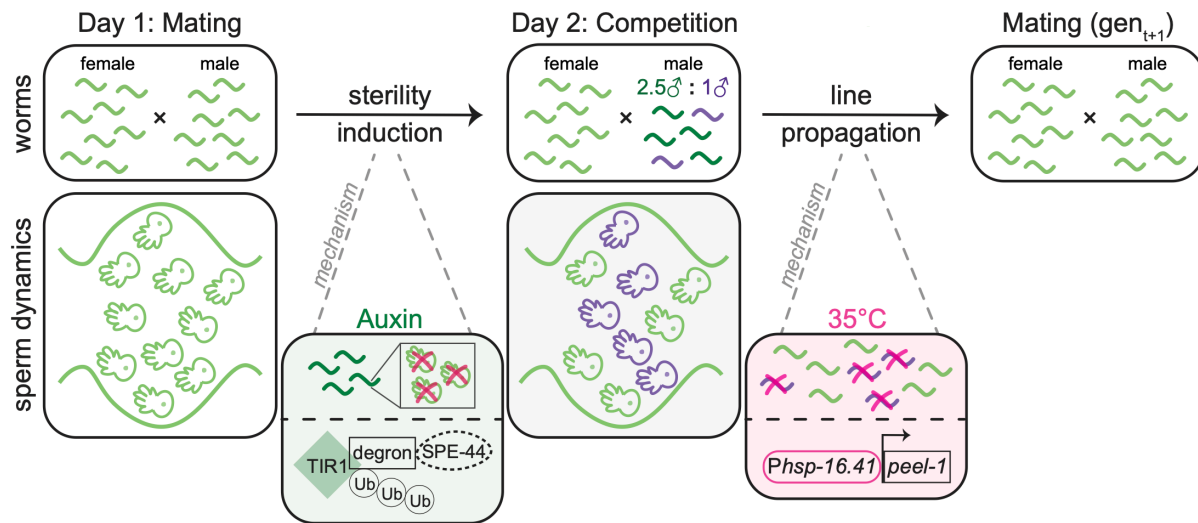
- 656 40. Hsu PD, Scott DA, Weinstein JA, Ran FA, Konermann S, Agarwala V, et al. DNA
657 targeting specificity of RNA-guided Cas9 nucleases. *Nat Biotechnol* 2016 34:3. 2013;31:
658 827–832.
- 659 41. Xu H, Xiao T, Chen C-H, Li W, Meyer CA, Wu Q, et al. Sequence determinants of
660 improved CRISPR sgRNA design. *Genome Res.* 2015;25: 1147–1157.
- 661 42. Dickinson DJ, Ward JD, Reiner DJ, Goldstein B. Engineering the *Caenorhabditis elegans*
662 genome using Cas9-triggered homologous recombination. *Nat Meth.* 2013;10: 1028–
663 1034.
- 664 43. Frøkjær-Jensen C, Davis MW, Ailion M, Jorgensen EM. Improved Mos1-mediated
665 transgenesis in *C. elegans*. *Nat Meth.* 2012;9: 117–118.
- 666 44. Paix A, Folkmann A, Rasoloson D, Seydoux G. High efficiency, homology-directed
667 genome editing in *Caenorhabditis elegans* using CRISPR-Cas9 ribonucleoprotein
668 complexes. *Genetics.* 2015;201: 47–54.
- 669 45. Stevenson ZC, Moerdyk-Schauwecker MJ, Jamison B, Phillips PC. Rapid self-selecting
670 and clone-free integration of transgenes into engineered crispr safe harbor locations in
671 *Caenorhabditis elegans*. *G3.* 2020;10: 3775–3782.
- 672 46. Brenner S. The genetics of *Caenorhabditis elegans*. *Genetics.* 1974;77: 71–94.
- 673 47. Kenyon C. The nematode *Caenorhabditis elegans*. *Science.* 1988;240: 1448–1453.
- 674 48. R Core Team. R: A language and environment for statistical computing [Internet]. Vienna,
675 Austria: Foundation for Statistical Computing; 2020. Available: [https://www.R-](https://www.R-project.org/)
676 [project.org/](https://www.R-project.org/)
- 677 49. Bates D, Mächler M, Bolker B, Walker S. Fitting linear mixed-effects models using lme4.
678 *J Stat Soft.* 2015;67: 1–48.
- 679 50. Hothorn T, Bretz F, Westfall P. Simultaneous inference in general parametric models.
680 *Biom J.* 2008;50: 346–363.
- 681 51. Jiang H, Lei R, Ding S-W, Zhu S. Skewer: a fast and accurate adapter trimmer for next-
682 generation sequencing paired-end reads. *BMC Bioinformatics.* 2014;15: 182–12.
- 683 52. Li H. Aligning sequence reads, clone sequences and assembly contigs with BWA-MEM.
684 arXiv. 2013;1303.3997v2: 1–3.
- 685 53. Li H, Handsaker B, Wysoker A, Fennell T, Ruan J, Homer N, et al. The Sequence
686 Alignment/Map format and SAMtools. *Bioinformatics.* 2009;25: 2078–2079.
- 687 54. Danecek P, Schiffels S, Durbin R. Multiallelic calling model in bcftools (-m). 2016.
688 Available at: <http://samtools.github.io/bcftools/call-m.pdf>

- 689 55. Begun DJ, Holloway AK, Stevens K, Hillier LW, Poh Y-P, Hahn MW, et al. Population
690 genomics: whole-genome analysis of polymorphism and divergence in *Drosophila*
691 *simulans*. PLoS Biol. 2007;5: e310.
- 692 56. Waples RS. A generalized approach for estimating effective population size from
693 temporal changes in allele frequency. Genetics. 1989;121: 379–391.
- 694 57. Jónás Á, Taus T, Kosiol C, Schlötterer C, Futschik A. Estimating the effective population
695 size from temporal allele frequency changes in experimental evolution. Genetics.
696 2016;204: 723–735.
- 697 58. UniProt Consortium. UniProt: the universal protein knowledgebase in 2021. Nucleic
698 Acids Res. 2021;49: D480–D489.
- 699 59. Huntley RP, Sawford T, Mutowo-Meullenet P, Shypitsyna A, Bonilla C, Martin MJ, et al.
700 The GOA database: gene ontology annotation updates for 2015. Nucleic Acids Res.
701 2015;43: D1057–63.

702

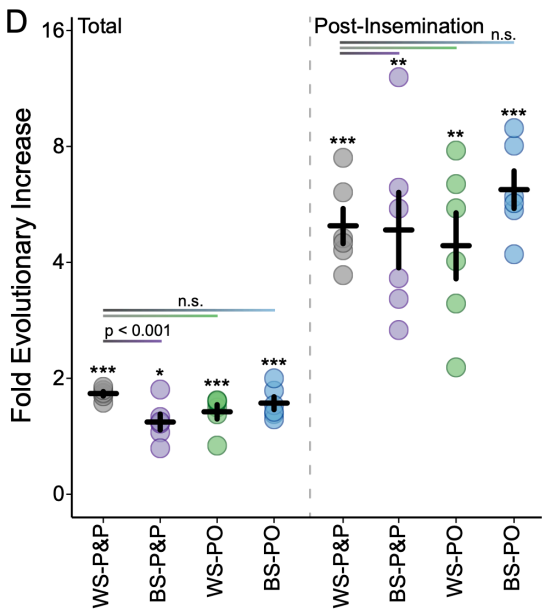
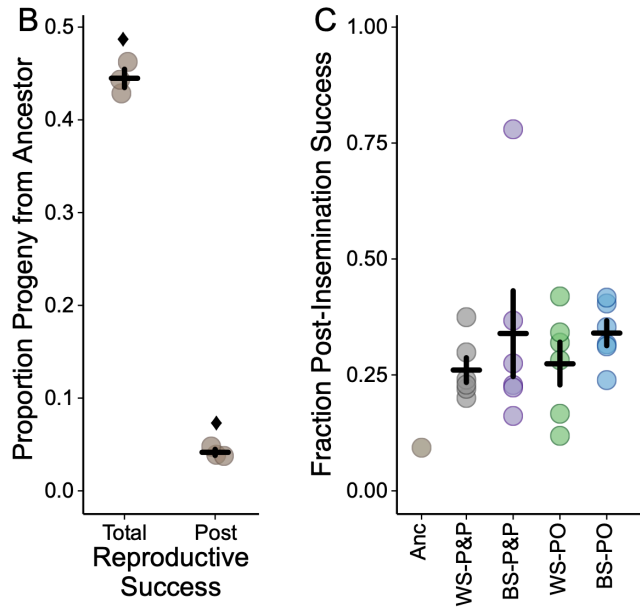
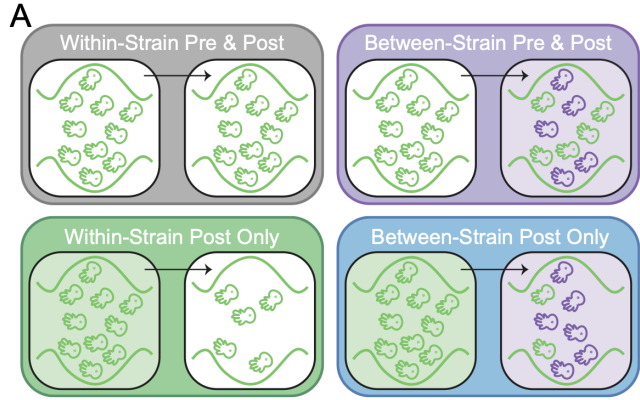
703 **Figures**

704

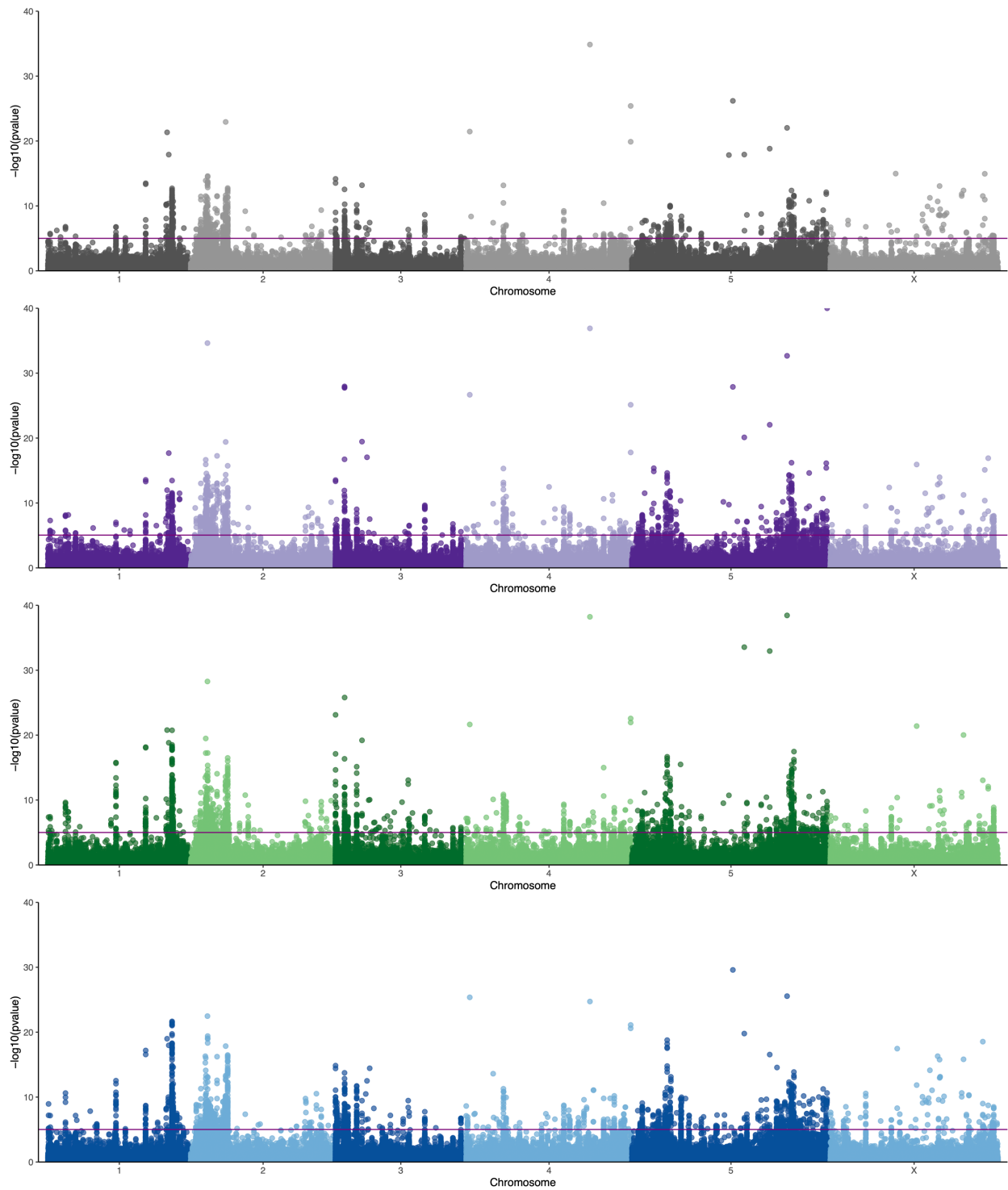


705

706 **Fig 1. Day-by-day depiction of the experimental evolution design shown at the population**
 707 **level and at the sperm level.** On day 1 sterility is induced by transferring worms to auxin-
 708 containing media. Auxin activates TIR1 to target the degron tag on SPE-44. The depletion of
 709 SPE-44 stops the production of sperm thereby inducing sterility. On day 2, competitor males are
 710 added to the population at a ratio of 1 competitor male to 2.5 evolving males. Progeny are
 711 collected on day 3 and heat-shocked on day 4 to induce ectopic expression of the toxic protein
 712 PEEL-1. This expression kills competitor cross-progeny, leaving only the progeny from sperm
 713 transferred during the day 1 mating phase. Each selective event is followed by a recovery
 714 generation.



716 **Fig 2. The competitive reproductive success of males before and after experimental**
717 **evolution under four sexual selection regimes. A)** Partitioning the sterility and competition
718 treatments leads to four experimental evolution regimes: within-strain pre- and post-insemination
719 competition (WS-P&P, gray), within-strain post-insemination only competition (WS-PO, green),
720 between-strain pre- and post-insemination competition (BS-P&P, purple), and between-strain
721 post-insemination only competition (BS-PO, blue). **B)** Ancestral males have poorer reproductive
722 success than competitor males under both pre- and post-insemination competitive conditions
723 (total) and under only post-insemination competitive conditions. Each point represents an
724 independent assay with the mean and standard error across assays given. Diamonds denote a
725 significant deviation from the null hypothesis of equal competitive ability between ancestral and
726 competitive males for each condition (total: $\chi^2 = 6.87$, d.f. = 1, $p < 0.01$, 95% C.I. of ancestral
727 competitive success = 40.4–48.6%; post-insemination: $\chi^2 = 863$, d.f. = 1, $p < 0.0001$, 95% C.I. of
728 ancestral sperm competitive success = 3.0–5.5%). **C)** The fraction of total reproductive success
729 attributable to post-insemination success in the ancestral population (Anc) and the evolved
730 populations (WS-P&P, BS-P&P, WS-PO, BS-PO). Each point represents a mean of three
731 independent assays for the ancestor and each evolved replicate with the mean and standard error
732 across evolved replicates shown. **D)** The fold change in the total reproductive success and the
733 post-insemination reproductive success of males in the evolved regimes relative to the ancestor
734 (plotted on a \log_2 scale). Males in all regimes significantly increased in both measures of
735 reproductive success (* $p < 0.05$, ** $p < 0.01$, *** $p < 0.001$). Post hoc tests for a difference
736 between the WS-P&P and the BS-P&P, WS-PO, and BS-PO regimes are indicated by the
737 horizontal lines. The only significant difference appears between the total reproductive success
738 of the WS-P&P and BS-P&P regimes, in which pre-insemination competition reduces the
739 evolutionary response. Each point represents a mean of three independent assays for each
740 evolved replicate with the mean and standard error across replicates shown.
741



742

743 **Fig 3. Genomic response for each SNP over time fit for each regime (Model 2).** The
 744 horizontal line represents the Bonferroni significance threshold. Reproductive success is a highly
 745 polygenic trait with 49 peaks identified in the WS-P&P regime (gray), 77 in the BS-P&P regime

746 (purple), 102 in the WS-PO regime (green), and 107 in the BS-PO regime (blue). The
747 distribution of peak overlaps is shown in Figure S3.

748 **Supporting information**

749 **S1 Fig. Schematic of strain construction.** **A)** The components for creating an obligate
750 outcrossing sterility induction line were genetically engineered in the wild isolate background
751 JU2526. The spermatogenesis gene *spe-44* was degraon-tagged and TIR1 was inserted to create
752 strain PX737. The hermaphrodite self-sperm gene (*fog-2*) was knocked-out to create strain
753 PX738. These strains are used in panels C and D. **B)** To generate an inducible lethality line, heat-
754 shock driven *peel-1* was inserted into the CB4856 background on Chromosomes I and II to
755 create strains PX739 and PX630, respectively. These strains are used in panels D and E. **C)**
756 Strains PX737 and PX738 were crossed to creating a male-female, inducible sterility triple
757 mutant (PX624). Strain PX624 went through five low dose rounds of mutagenesis each followed
758 by two recovery generations. After the final recovery generation, the population was expanded
759 for 15 generations of lab adaptation to create the experimental evolution ancestral population
760 (PX632). **D)** The competition strain has five transgenic modifications. Heat-shock driven *peel-1*
761 was inserted on Chromosome III of strain PX737, creating an inducible lethality and inducible
762 sterility strain (PX656). Strains PX624 and PX631 (panel E) were crossed to given another
763 inducible lethality and sterility double mutant. These worms were backcrossed to PX624 five
764 times to give a predominantly JU2526 genomic background. This strain, PX655, was crossed
765 with PX656 yielding a quintuple mutant, which was inbred to three generations followed by five
766 generations of lab adaptation. The final strain PX658 served as the competitor during
767 experimental evolution. **E)** A separate bioassay competitor strain was generated by introgressing
768 the *fog-2*(q71) mutation into PX739. These worms were backcrossed to the CB4856 genomic
769 background four times and then inbred for 14 generations, creating strain PX626. This strain was
770 crossed to PX630 to create an obligate outcrossing strain with two heat-shock driven *peel-1*
771 insertions. The final strain PX631 served as the novel competitor during phenotypic assays.

772
773 **S2 Fig. Genetic diversity of the ancestral population.** **A)** The minor allele frequency (MAF)
774 across Chromosome II (as an exemplar). The genome-wide mean is shown in blue. **B)** Histogram
775 of MAF counts across the entire genome binned by chromosome arms and chromosome center.
776 Values of zero are excluded from the plot. **C)** Nucleotide diversity (π) calculated per SNP across
777 Chromosome II. The genome-wide mean is shown in blue. **D)** Histogram of nucleotide diversity
778 across the entire genome binned by chromosome arms and chromosome center. Values of zero

779 are excluded from the plot. **E)** SNP density (θ_w) per base pair across Chromosome II. The
780 genome-wide mean is shown in blue. **F)** Histogram of SNP density in 1kb windows across the
781 entire genome binned by chromosome arms and chromosome center.

782

783 **S3 Fig. The estimated effective population size (N_e) per chromosome for all replicates.** The
784 effective population size was greatly reduced compared to the census size ($N = 5,000$). Regime
785 did not have a significant effect on effective population size ($F = 0.72$, d.f. = 3, $p = 0.54$).

786

787 **S4 Fig. Breakdown of significance peaks from Model 2.** The counts of significance peaks are
788 shown along with the combination of regimes contributing to that count. Unique peaks are
789 represented by a single black dot for the given regime. Shared peaks have multiple connected
790 black dots. The total number of significant SNPs within each regime is given.

791

792 **S5 Fig. Zoom plot of the major significance peak on the right arm of Chromosome I.**
793 Significant SNPs pile up in the second intron of gene C17H1.2. This gene has male-biased
794 expression, though it's function is uncharacterized.

795

796 **S6 Fig. The molecular functions for genes associated with significance peaks based on a GO**
797 **analysis.** Ubiquitin ligase complex formation through F-box proteins, carbohydrate binding, G-
798 coupled protein receptor activity, and transferase transporter activity were the most common
799 functions identified. However, the majority of genes are yet uncharacterized in function.

800

801 **S1 Table. Guide sequences.** The guide sequence, genomic location, target region/gene, and
802 format (plasmid or cr:tracrRNA) are given.

803

804 **S2 Table. Plasmid construction.** The plasmid name and insert are given for both plasmids used
805 in construction and as repair templates.

806

807 **Table S3. Primers.** The primer name, sequence (in 5' to 3' orientation), and purpose for a given
808 primer are listed.

809

810 **Table S4. Strains generated in this study.** Full genotype information for each strain used in
811 this study, along with the genomic background, method of construction, and generations of
812 backcrossing and/or inbreeding.

813

814 **S1 File. SNP data for the ancestor.** The chromosome, position (in base pairs), reference allele,
815 alternate allele, counts of reference alleles, counts of alternate alleles, total coverage, minor allele
816 frequency (MAF), chromosome domain, and nucleotide diversity (π) are given.

817

818 **S2 File. Watterson's theta calculated in 1kb windows across each chromosome.** The
819 chromosome, chromosome domain, theta per window, and theta per base pair are given.

820

821 **S3 File. Effective population size estimated using Waples Plan II sampling for each
822 replicate and each chromosome.**

823

824 **S4 File. Summary statistics for the Model 1 planned comparison analysis of ancestral
825 versus evolved allele counts.** For each SNP, the chromosome and position (in base pairs) is
826 given along with the slope estimate and p-value for each regime comparison.

827

828 **S5 File. Summary statistics for the Model 2 GLM analysis of allele counts over time for
829 each regime.** For each SNP within each regime, the chromosome and position (in base pairs) is
830 given along with the model intercept, slope estimate, standard error, z-value, and p-value.

831

832 **S6 File. Summary of the significance peaks identified using the Model 2 genomic results.**
833 The chromosome, start position (in base pairs), stop position (in base pairs), presence in each
834 treatment, associated gene, genetic region, molecular function (from GO analysis), and
835 biological function (from GO analysis) are given.

836

837 **S7 File. Competitive phenotyping data for the ancestor and all evolved replicates.**





[Click here to access/download](#)

**Supporting Information - Compressed/ZIP File Archive
Supplemental Tables.zip**

